Effects of integrin $\alpha_v\beta_3$ on differentiation and collagen synthesis induced by connective tissue growth factor in human hypertrophic scar fibroblasts

XIAOLONG HU*, NA LI*, KE TAO*, XIAOBING FANG, JIAQI LIU, YAOJUN WANG, HONGTAO WANG, JIHONG SHI, YUNCHUAN WANG, PENG JI, WEIXIA CAI, XIAOZHI BAI, XIONGXIANG ZHU, JUNTAO HAN and DAHAI HU

Department of Burns and Cutaneous Surgery, Xijing Hospital, Fourth Military Medical University, Xi'an, Shaanxi 710032, P.R. China

Received January 6, 2014; Accepted August 12, 2014

DOI: 10.3892/ijmm.2014.1912

Abstract. CCN2 is a matricellular protein that appears to be important in scar formation. CCN2 mediates the pro-fibrotic effects in hypertrophic scars (HTSs) through an unknown mechanism. However, many activities of CCN2 protein are known to be mediated by direct binding to integrin receptors. In this study, we investigated the role of integrin $\alpha_v\beta_3$ in the differentiation of hypertrophic scar fibroblasts (HTSFs) induced by CCN2. The levels of integrin $\alpha_v\beta_3$ between normal skin and hypertrophic scar (HTS) tissues were compared, and integrin $\alpha_v\beta_3$ was found to be upregulated in HTS. CCN2 was shown to induce HTSF differentiation and collagen (COL) synthesis at the mRNA and protein levels. Based on these results, the expression of integrin $\alpha_v\beta_3$ was upregulated by CCN2 stimulation during HTSF differentiation. Blockade of integrin $\alpha_v\beta_3$ prevented CCN2-induced HTSF differentiation and COL synthesis. Furthermore, the CCN2-induced increase in contractility of the HTSF in COL lattices was inhibited by integrin $\alpha_v\beta_3$ blocking antibodies. HTSs were established in a rabbit ear model, and the inhibitor of integrin $\alpha_v\beta_3$ significantly improved the architecture of the rabbit ear scar. Results of the present study showed that integrin $\alpha_v\beta_3$ contributes to pro-fibrotic CCN2 signaling. Blocking this pathway may therefore be beneficial for the treatment of HTS.

Introduction

Over 70% of patients with burn injuries develop hypertrophic scarring (HTS), which may manifest as tissue disfigurement or disruption of normal physiologic and/or physical function. There is currently no effective and safe strategy for the prevention or inhibition of HTS formation (1). Therefore, investigations on how to reduce HTS occurrence during the skin wound-healing process is of great clinical value.

CCN2, also known as connective tissue growth factor, plays an important role in promoting fibrosis and scarring in numerous tissues (2,3). CCN2 has been characterized as a cysteine-rich protein that stimulates a broad repertoire of cell responses, including proliferation, migration, adhesion, matrix production and differentiation (4). Overexpression of CCN2 has been shown to promote fibrosis and scar formation in skin, kidney, liver, brain, lung, vasculature and pancreas (3,5,6).

Previous studies have provided strong evidence of a role for CCN2 in HTS, especially as a cofactor of transforming growth factor β1 (TGF-β_1) function (7,8). Several cell types have been shown to produce CCN2 in HTS (9-11), with attention being focused on hypertrophic scar fibroblasts (HTSFs). Baseline CCN2 expression is increased in unstimulated HTSF, as compared to that in normal fibroblasts, and HTSF production is increased by the CCN2-stimulated activation of TGF-β_1 (9). CCN2 also plays a critical role in mediating many of the important fibroproliferative effects of TGF-β_1 (12). Furthermore, antisense oligonucleotides targeting CCN2 have no measurable effect on early wound closure events but significantly decrease the transcription of TIMP-1 and collagen (COL) types I and III in rabbit models (13). Therefore, understanding the regulatory mechanisms of CCN2 may benefit therapeutic efforts to inhibit HTS.

In recent years, progress has been made in determining the mechanisms that underlie the diverse effect of CCN2 proteins on cell function. However, the specific mechanisms involved in the CCN2-dependent fibrogenic response remain to be clarified. In general, the intracellular signaling pathways activated by CCN2 remain unknown because the bona fide CCN2 receptor has yet to be identified. Findings of a recent study have shown that many activities of CCN2 proteins are mediated by directly binding to integrin receptors (2).

Integrin $\alpha_v\beta_3$ cluster with the TGF-β type II receptor and mediate TGF-β-induced proliferation of human lung

Correspondence to: Professor Dahai Hu, Department of Burns and Cutaneous Surgery, Xijing Hospital, Fourth Military Medical University, 127 Changle West Road, Xi'an, Shaanxi 710032, P.R. China
Email: hudhai@fmmu.edu.cn

*Contributed equally

Key words: connective tissue growth factor, integrin, differentiation, collagen synthesis, hypertrophic scar

Table I. Demographic data of patient samples used in the present study.

Patient no.	Diagnosis	Age (years)	Gender	Duration (months)	Ethnicity
1	Hypertrophic scar	35	Female	3	Chinese
2	Hypertrophic scar	40	Male	10	Chinese
3	Hypertrophic scar	20	Male	6	Chinese
4	Hypertrophic scar	29	Female	8	Chinese
5	Hypertrophic scar	41	Male	5	Chinese
6	Hypertrophic scar	36	Male	12	Chinese

fibroblasts (14). Moreover, integrin $\alpha_v\beta_3$ appear to mediate the profibrotic effects of TGF-β in scleroderma fibroblasts (15). Previous studies have shown that integrin $\alpha_v\beta_3$ is crucial in several processes related to tissue remodeling, such as the binding and activation of matrix metalloproteinases and growth factors, as well as cell proliferation, migration and differentiation (16-19). However, the potential for integrin $\alpha_v\beta_3$ to interact with CCN2 in HTS remains unclear.

Based on the previous findings in the literature, we hypothesized that integrin $\alpha_v\beta_3$ mediates COL synthesis and HTSF differentiation in HTS. In this study, we investigated whether CCN2 induced HTSF differentiation and COL synthesis. The expression levels of integrin $\alpha_v\beta_3$ in normal, undamaged skin was compared to that in HTS. An *in vitro* and *in vivo* HTS model was used to investigate the effect of integrin $\alpha_v\beta_3$ on COL synthesis and HTSF differentiation.

Materials and methods

Reagents. Recombinant human CCN2 (rhCCN2) was obtained from PeproTech (London, UK). Dulbecco's modified Eagle's medium (DMEM) was purchased from Gibco (Grand Island, NY, USA). Blocking antibody targeting integrin $\alpha_v\beta_3$ were obtained from Millipore Biotechnology (Temecula, CA, USA). Murine polyclonal antibody against COL type IA2 and goat polyclonal antibody against COL type IIIA1 were purchased from Santa Cruz Biotechnology, Inc. (Santa Cruz, CA, USA). Murine monoclonal antibody against α-smooth muscle actin (SMA) and rabbit polyclonal antibody against β-actin were obtained from Boster Biological Technology Co. (Wuhan, China). Cy3-conjugated goat anti-mouse IgG antibodies were purchased from Cwbio (Beijing, China). Inhibitor of activin receptor-like kinase (ALK)5 (the TGF-β type I receptor) was purchased from Selleck (SB431542). Polyvinylidene fluoride (PVDF) membranes and Immobilon Western chemiluminescent horseradish peroxidase (HRP) substrate were purchased from Millipore Co. (Bedford, MA, USA).

Cell culture and treatment. Normal skin and hypertrophic scar tissues were obtained from patients who underwent plastic surgery at the Xijing Hospital (Xi'an, China). Each patient demonstrated extensive areas of HTS, which manifested as raised, erythematous, pruritic and thickened scars restricted to the injury site. The demographic data of the patients enrolled in the present study are shown in Table I. Specimens were obtained from the Human Subjects Committee of the local institution. Dermal portions were minced and incubated in a solution of collagenase type I (0.1 mg/ml) at 37˚C for 3 h to separate the fibroblasts. The fibroblasts were pelleted and grown in DMEM supplemented with 10% fetal calf serum (Gibco), 100 U/ml penicillin, and 100 U/ml streptomycin at 37˚C in a 5% (v/v) CO_2 humidified atmosphere. Cells between the third and sixth sub-passages were used for subsequent experiments.

The fibroblasts were seeded in 60-mm culture dishes and grown to 80-90% confluence. Prior to treatment, the cells were cultured in serum-free DMEM for 12 h. The cells were then treated in the absence or presence of integrin $\alpha_v\beta_3$ antibody (LM609, 10 μg/ml) or ALK5 inhibitor (SB431542, 10 μM) for 1 h. CCN2 (5-80 ng/ml) and/or TGF-β_1 (10 ng/ml) were subsequently added to the culture for a time period determined by the specific experiment. The cells of the control group were added to an equal volume of serum-free medium. The culture media and cells were harvested and analyzed at time points indicated in each experiment to measure RNA and protein levels.

Rabbit ear model of hypertrophic scar tissue and treatment. A model for hypertrophic scar in rabbit was used as previously described (7). New Zealand white rabbits were anaesthetized by the intravenous administration of sodium pentobarbital (30 mg/kg). Six 10-mm dermal wounds were created on the ventral surface of each ear down to bare cartilage after removal of the perichondrium. On postoperative day 29 and afterwards, scars were randomly classified into five groups (n=18 scars per group): one control group, one PBS group and three treatment groups. CCN2 (40 ng/ml), integrin $\alpha_v\beta_3$ antibody (LM609, 10 μg/ml) and CCN2 (40 ng/ml) + integrin $\alpha_v\beta_3$ antibody (LM609, 10 μg/ml), respectively, were applied once daily to the scars.

RNA isolation and quantitative PCR. Quantitative PCR (qPCR) was performed as previously reported (20). Briefly, total RNA was isolated with the TRIzol reagent (Invitrogen Life Technologies, Carlsbad, CA, USA) according to the manufacturer's instructions. Total RNA was reverse transcribed using the PrimeScript RT kit (Takara, Dalian, China) according to the manufacturer's instructions. qPCR was carried out with the Bio-Rad IQ^5 Real-Time System (Bio-Rad, Hercules, CA, USA) using the SYBR® Premix Ex*Taq*™ II kit (Takara). Primer sequences were: α-SMA, forward 5'-GAC AATGGCTCTGGGCTCTGTAA-3' and reverse 5'-TGTGCT

TCGTCACCCACGTA-3'; COL A2, forward 5'-GAGGGCAAC AGCAGGTTCACTTA-3' and reverse 5'-TCAGCACCACCG ATGTCCA-3'; COL IIIA1, forward 5'-CCACGGAAACAC TGGTGGAC-3' and reverse 5'-GCCAGCTGCACATCAAG GAC-3'; integrin α_v, forward 5'-AGCTGAGCTCATCGTTTC CATTC-3' and reverse 5'-CCTTCATTGGGTTTCCAA GGTC-3'; integrin β_3, forward 5'-GAGGTCATCCCT GGCCTCAA-3' and reverse 5'-CTGGCAGGCACAGTC ACAATC-3'; CCN2, forward 5'-CTTGCGAAGCTGACC TGGAA-3' and reverse 5'-AGCTCAAACTTGATAGGCTTG GAGA-3'; GAPDH, forward 5'-GCACCGTCAAGGCTG AGAAC-3' and reverse 5'-TGGTGAAGACGCCAGTGGA-3'. qPCRs were performed in triplicate. Gene expression levels were normalized against the expression level of the housekeeping gene GAPDH.

Western blot analysis. Western blotting was performed as previously described (21). Briefly, 50 μg protein samples were resolved by sodium dodecyl sulfate-polyacrylamide gel electrophoresis (SDS-PAGE), and then transferred to a PVDF membrane. The membranes were blocked with 5% non-fat milk, and incubated with antibodies for murine anti-human COL type IA2 (1:200), goat anti-human COL type IIIA1 (1:200), rabbit anti-human β-catenin (1:700) or murine anti-human α-SMA (1:350) overnight at 4˚C. HRP-conjugated goat anti-rabbit IgG (1:3,000), goat anti-mouse IgG (1:3,000) or rabbit anti-goat IgG (1:3,000) were used as secondary antibodies. Proteins were visualized by an enhanced chemiluminescence system using FluorChem FC (Alpha Innotech, San Leandro, CA, USA).

Immunocytochemistry. Immunocytochemistry was performed as previously reported (7). Cell samples were fixed with 90% ethanol and blocked with 3% bovine serum albumin. The samples were incubated with murine anti-α-SMA antibodies at a dilution of 1:100. After being washed with PBS, the samples were incubated with Cy3-conjugated goat anti-murine IgG antibody at a dilution of 1:50. The samples were subsequently stained with 4',6'-diamidino-2-phenylindole (DAPI). The coverslips were subsequently mounted onto glass slides and viewed with Olympus Box-Type Photofluorography Unit Model FSX100. DAPI-positive and α-SMA-positive cells were counted on the slide at three randomly selected regions. Fluorescence was analyzed by Image-Pro Plus system.

Fibroblast-populated COL lattices contraction and improvement assays. Type I COL was extracted from rat-tail tendons as described by Bell *et al* (22). The HTSF-populated COL lattices contractility assays were performed in 24-well plates. A 0.5 ml suspension containing $1x10^5$ cells, 1.4 mg/ml COL, CCN2 and integrin $\alpha_v\beta_3$ antibody (LM609) was added to the triplicate wells and incubated at 37˚C for 1 h to allow the mixture to gel. DMEM (1 ml) supplemented with either CCN2 (40 ng/ml), LM609 (10 μg/ml), or both was added and stirred gently. The gels were incubated at 37˚C for 24 h, followed by mechanical detachment from the side of the wells. Images were captured at 0 and 48 h after the gels were released. The surface areas of the gels at each time point were measured using Image ProPlus 6.0 software, and were normalized by the surface area and then measured immediately after detachment.

After detachment from the side of the wells at 48 h, fibroblast-populated COL lattices were fixed with 4% paraformaldehyde in PBS overnight. The sections were stained with hematoxylin and eosin (H&E) and analyzed using the framework of FPCL by FSX100.

Masson's trichrome staining for COL fibers. Masson's trichrome staining analysis of COL fibers was performed as previously described (7). Briefly, the samples were rehydrated through gradient ethanol immersion. The tissues were subsequently stained by placing them in Weigert's iron hematoxylin working solution. The slides were then stained in Biebrich scarlet-acid fuchsin solution, and placed in 1% phosphomolybdic-phosphotungstic acid solution. The sections were directly transferred into aniline blue solution and rinsed in 1% acetic acid solution. The tissue samples were then dehydrated, cleared, and mounted. A bluestain indicated the presence of COL fibers. The histologic characteristics and the COL fibers in the samples were observed under FSX100.

Statistical analysis. Results are presented as mean ± standard error of three independent experiments. Statistical analysis was performed by analysis of variance (ANOVA). The paired-samples t-test was used for comparison of gene expression levels between scar and normal skin samples. $P<0.05$ was considered to indicate a statistically significant result.

Results

Expression levels of CCN2, COL IA2 and COL IIIA1 mRNA in normal skin and HTS. As an initial experiment, we compared the transcript levels of CCN2, COL IA2 and COL IIIA1 between normal and HTS skin *in vivo*. Total RNA was extracted from the scar and normal skin tissues derived from six patients with HTS, and qPCR was performed. The relative transcript levels of CCN2, COL IA2 and COL IIIA1 were significantly higher in HTS skin than those in the control skin (Fig. 1).

Expression levels of CCN2, COL IA2 and COL IIIA1 mRNA in cultured normal and HTSF. Cultured human dermal fibroblasts obtained from normal and HTS skin were incubated under the same conditions, and their mRNA expression was analyzed. The expression of CCN2, COL IA2 and COL IIIA1 mRNA was upregulated in HTSF (Fig. 2), which was consistent with the *in vivo* results.

Expression levels of integrin α_v and β_3 mRNA in normal skin and HTS. Subsequently, we compared the transcript levels of integrin α_v and β_3 between normal and HTS skin *in vivo*. Total RNA was extracted from the scar and normal skin tissues derived from six patients with HTS, and qPCR was performed. The relative transcript levels of integrin α_v and β_3 were significantly lower in the normal skin samples. By contrast, the integrin α_v and β_3 expression levels were significantly higher in the HTS skin than those in the control skin (Fig. 3).

Expression levels of integrin α_v and β_3 mRNA in cultured normal and HTSF. Cultured human dermal fibroblasts obtained from normal and HTS skin were incubated under the same conditions, and their mRNA expression was analyzed.

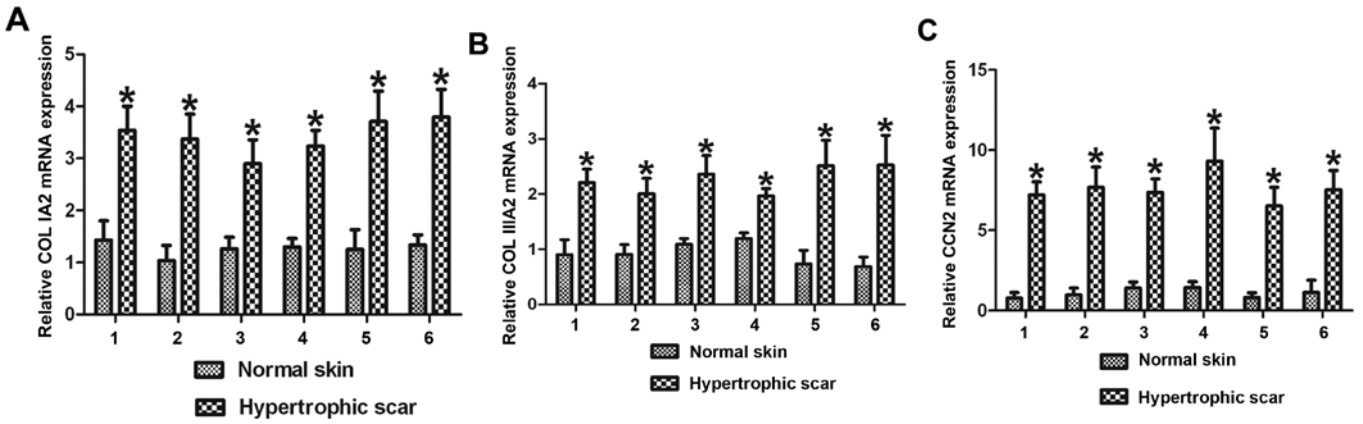

Figure 1. Expression of CCN2, collagen (COL) IA2 and COL IIIA1 was determined by qPCR analysis in normal skin and hypertrophic scar (HTS). (A) COL IA2 mRNA expression levels were detected by qPCR. (B) COL IIIA1 levels were measured by real time PCR. (C) CCN2 expression levels were detected by qPCR. Data are representative of three independent experiments. *P<0.05 vs. normal skin.

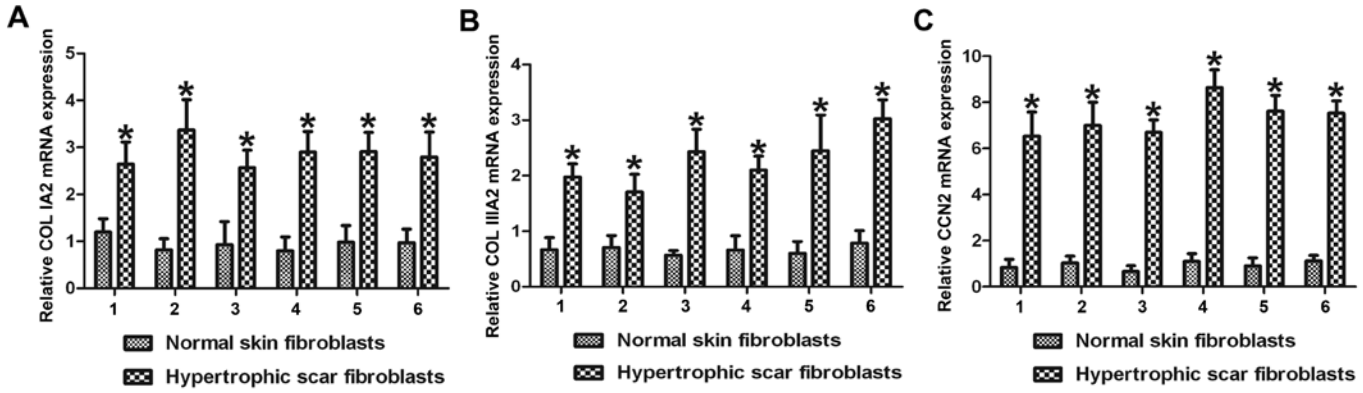

Figure 2. Expression of CCN2, collagen (COL) IA2 and COL IIIA1 was determined by qPCR analysis in cultured normal and hypertrophic scar fibroblasts (HTSFs). (A) COL IA2 mRNA expression levels were detected by qPCR. (B) COL IIIA1 levels were measured by qPCR. (C) CCN2 expression levels were detected by qPCR. Data are representative of three independent experiments. *P<0.05 vs. normal dermal fibroblasts.

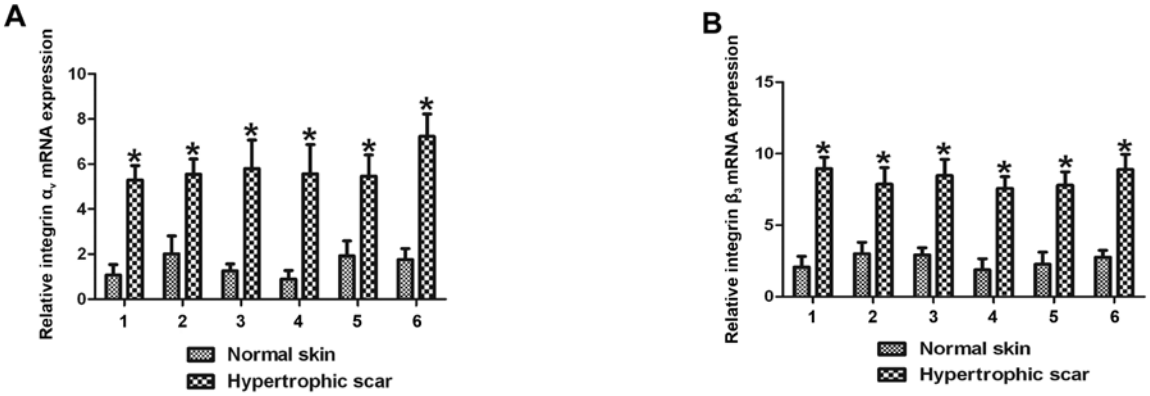

Figure 3. Expression of integrin α_v and integrin β_3 was determined by qPCR analysis in normal skin and hypertrophic scar (HTS). (A) Integrin α_v mRNA expression levels were detected by qPCR. (B) Integrin β_3 levels were measured by qPCR. Data are representative of three independent experiments. *P<0.05 vs. normal skin.

The expression of integrin α_v and β_3 mRNA was also upregulated in HTSF (Fig. 4), which was consistent with the *in vivo* results.

CCN2 induces HTSF differentiation and COL synthesis. Myofibroblasts play a key role in the wound-healing process, promoting wound closure and matrix deposition.

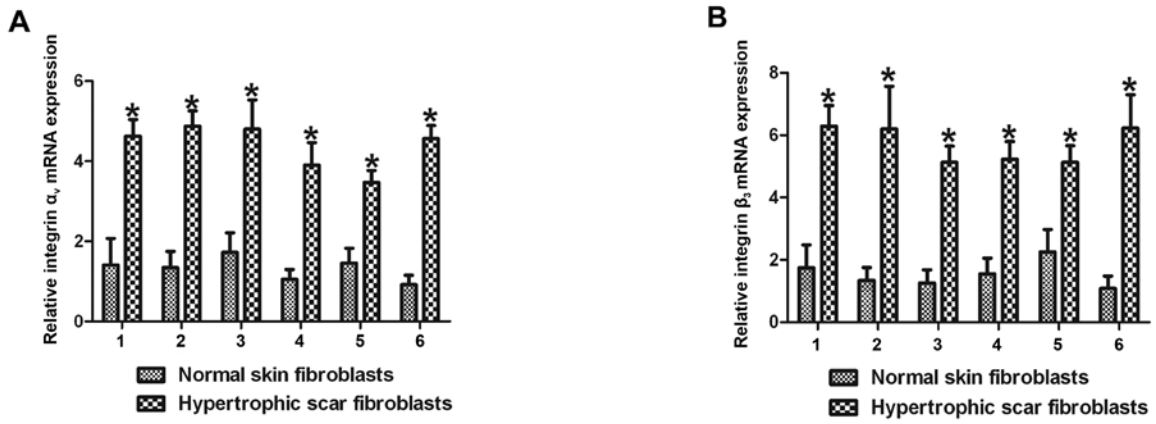

Figure 4. Expression of integrin α_v and β_3 was determined by qPCR analysis in cultured normal and hypertrophic scar fibroblasts (HTSFs). (A) Integrin α_v mRNA expression levels were detected by qPCR. (B) integrin β_3 levels were measured by qPCR. Data are representative of three independent experiments. *P<0.05 vs. normal dermal fibroblasts.

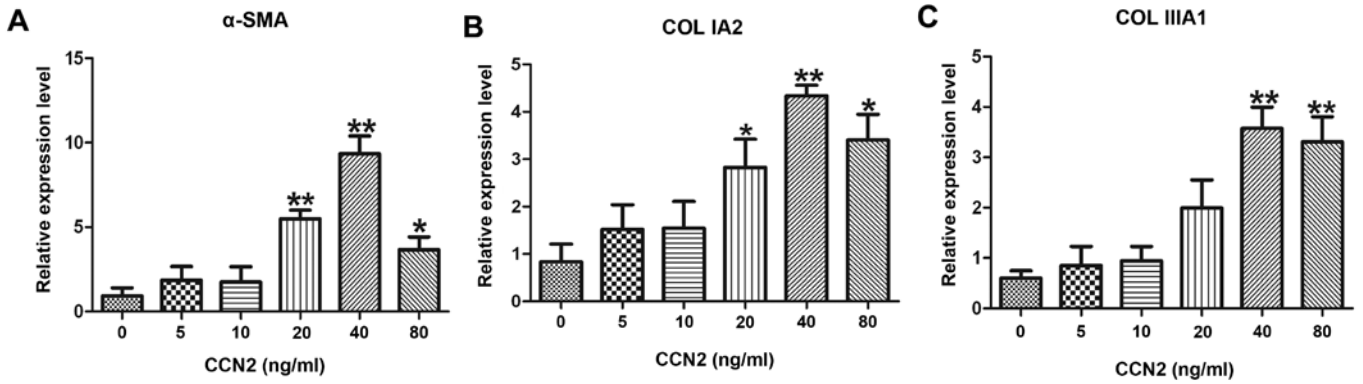

Figure 5. Expression mRNA levels of α-smooth muscle actin (SMA), collagen (COL) IA2, and COL IIIA1 after CCN2 stimulation in hypertrophic scar fibroblasts (HTSFs). HTSFs were incubated with 5-80 ng/ml CCN2 for 24 h. The expression of α-SMA, COL IA2 and COL IIIA1 mRNA were analyzed by qPCR and normalized to GAPDH. (A) α-SMA, (B) COL IA2 and (C) COL IIIA1. Data are representative of three independent experiments. *P<0.05 vs. control cells without CCN2 stimulation, **p<0.01 vs. control cells without CCN2 stimulation.

The differentiation of fibroblasts into myofibroblasts can be identified by the expression of α-SMA, which is organized into stress fibers. The regulation of myofibroblast differentiation is crucial because an excessive number of myofibroblasts is associated with increased pathologic scar formation (23). CCN2 has an established role in regulating the extracellular matrix (ECM). Then, we evaluated the effects of CCN2 on the differentiation and COL synthesis of HTSF. The mRNA levels of α-SMA, COL IIIA1 and COL IA2 increased gradually after rCCN2 stimulation in a dose-dependent manner and peaked with 40 ng/ml (Figs. 5 and 6). Similarly, the protein levels of α-SMA, COL IA2 and COL IIIA1 increased after rCCN2 stimulation and peaked with 40 ng/ml.

CCN2 increases integrin α_v and β_3 mRNA expression in HTSF. To determine whether CCN2 altered the cellular surface expression of integrin α_v and β_3 on HTSF, HTSFs were treated with CCN2 and integrin α_v or β_3 mRNA expression was measured. The cells were treated with 5-80 ng/ml CCN2 for 24 h. CCN2 gradually increased the transcription of integrin α_v and β_3 mRNA, which peaked at CCN2 (40 ng/ml) (Fig. 7).

Functional blockade of integrin $\alpha_v\beta_3$ blocks CCN2-induced HTSF differentiation and COL synthesis. To investigate whether integrin $\alpha_v\beta_3$ was required for CCN2-induced α-SMA and COL I expression, HTSFs were treated with or without LM609. α-SMA, COL IA2 mRNA and protein expression was then measured. Treatment with LM609 significantly inhibited α-SMA and COL IA2 mRNA expression (Fig. 8). Similarly, the expression of α-SMA COL IA2 protein was significantly decreased in the presence of LM609 (Fig. 9). Immunocytochemistry also showed that the expression of α-SMA by CCN2 was significantly decreased after the presence of LM609 (Fig. 10).

HTSF is controlled by blockage of the intergrin receptor following TGF-β_1 stimulation. PCR and WB for α-SMA, COL I and COL III in HTSFs treated with different receptor inhibitors after TGF-β_1 stimulation were conducted. Compared with the control, TGF-β_1 markedly stimulated α-SMA COL I and COL III expression, while treatment with the ALK5 (SB-431542) and $\alpha_v\beta_3$ integrin-specific (LM609) inhibitor suppressed the TGF-β_1-induced expression of α-SMA COL I

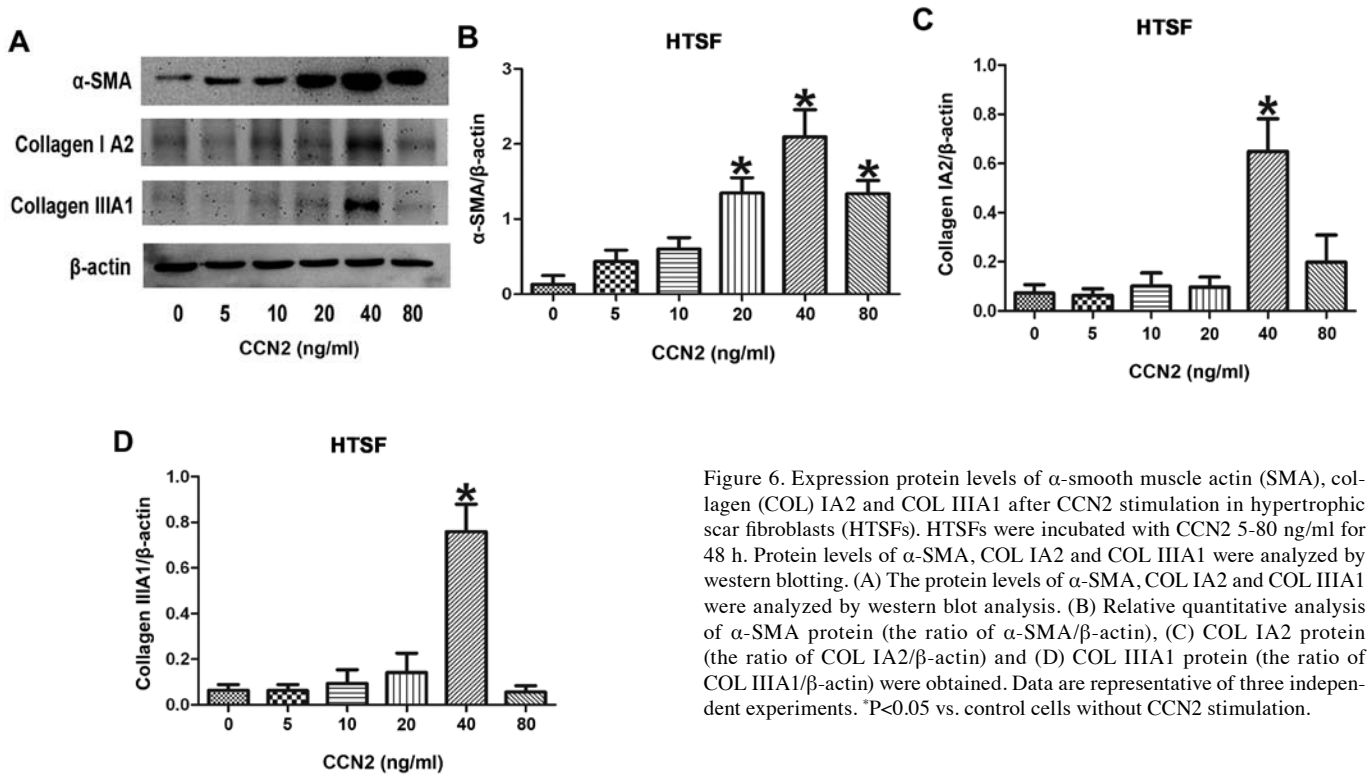

Figure 6. Expression protein levels of α-smooth muscle actin (SMA), collagen (COL) IA2 and COL IIIA1 after CCN2 stimulation in hypertrophic scar fibroblasts (HTSFs). HTSFs were incubated with CCN2 5-80 ng/ml for 48 h. Protein levels of α-SMA, COL IA2 and COL IIIA1 were analyzed by western blotting. (A) The protein levels of α-SMA, COL IA2 and COL IIIA1 were analyzed by western blot analysis. (B) Relative quantitative analysis of α-SMA protein (the ratio of α-SMA/β-actin), (C) COL IA2 protein (the ratio of COL IA2/β-actin) and (D) COL IIIA1 protein (the ratio of COL IIIA1/β-actin) were obtained. Data are representative of three independent experiments. *P<0.05 vs. control cells without CCN2 stimulation.

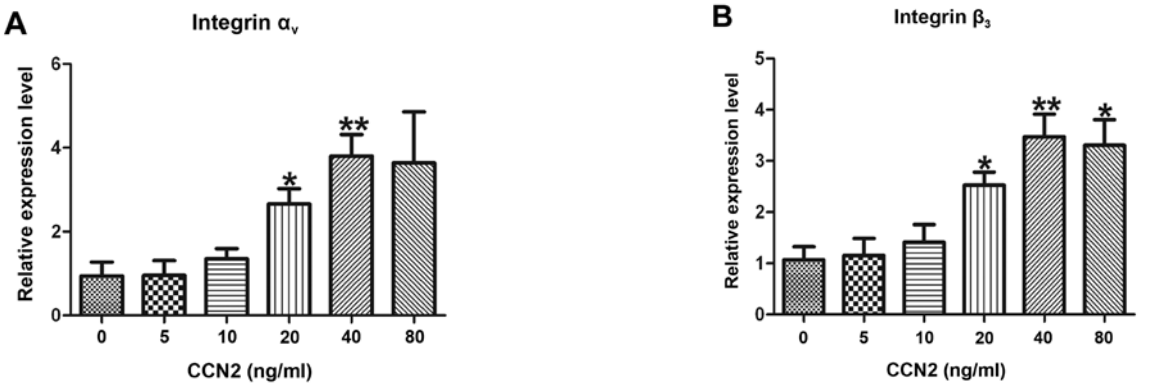

Figure 7. Expression levels of integrin α_v and β_3 following CCN2 stimulation in hypertrophic scar fibroblasts (HTSFs). HTSFs were incubated with 5-80 ng/ml CCN2 for 24 h. The expression of integrin α_v and β_3 mRNA was analyzed by qPCR and normalized to GAPDH. Integrin (A) α_v, and (B) β_3. Data are representative of three independent experiments. *P<0.05 vs. control cells without CCN2 stimulation, **p<0.01 vs. control cells without CCN2 stimulation.

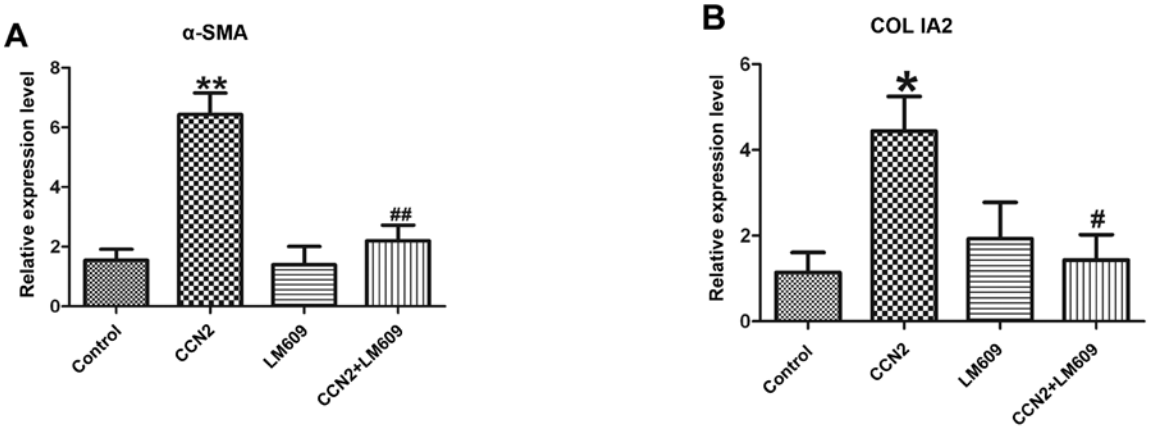

Figure 8. LM609 inhibits the expression mRNA levels of α-smooth muscle actin (SMA), collagen (COL) IA2 in hypertrophic scar fibroblasts (HTSFs) induced by CCN2. HTSFs were pretreated with integrin $\alpha_v\beta_3$ antibody (LM609, 10 μg/ml) for 1 h. Subsequently, they were treated with CCN2 (40 ng/ml) for 24 h. Expression of α-SMA and COL IA2 was determined by qPCR. (A) α-SMA and (B) COL IA2. Data are representative of three independent experiments. *P<0.05 vs. control, **p<0.01 vs. control; #p<0.05 vs. CCN2 group, ##p<0.01 vs. CCN2 group.

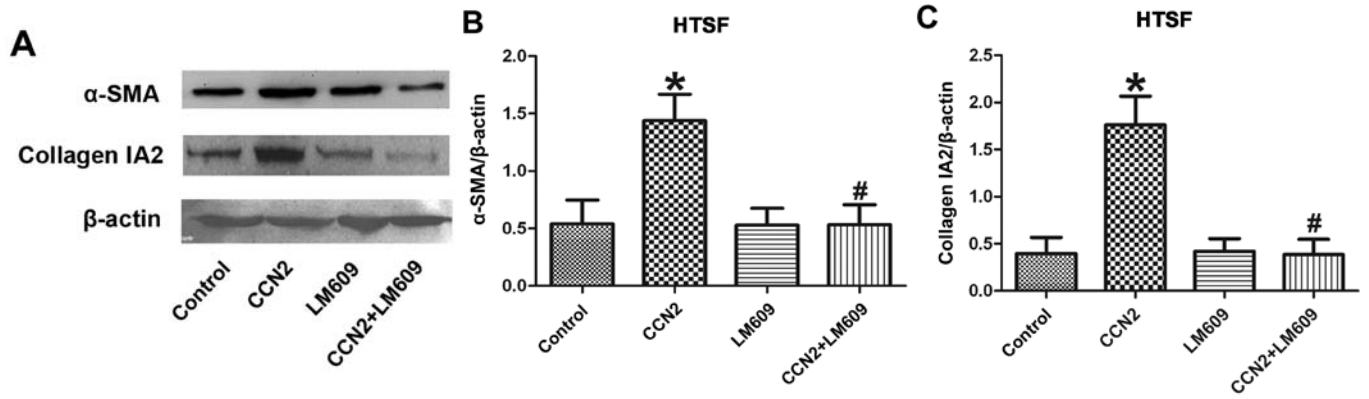

Figure 9. LM609 inhibits the expression protein levels of α-smooth muscle actin (SMA), collagen (COL) IA2 in hypertrophic scar fibroblasts (HTSFs) induced by CCN2. HTSFs were pretreated with integrin $\alpha_v\beta_3$ antibody (LM609, 10 μg/ml) for 1 h. Subsequently, they were treated with CCN2 (40 ng/ml) for 48 h. Expression of α-SMA and COL IA2 was determined by western blot analysis. (A) The protein levels of α-SMA and COL IA2 were analyzed by western blot analysis. (B) Relative quantitative analysis of α-SMA protein (the ratio of α-SMA/β-actin) and (C) COL IA2 protein (the ratio of COL IA2/β-actin) was obtained. Data are representative of three independent experiments. *P<0.05 vs. control; $^{\#}$p<0.05 vs. CCN2 group.

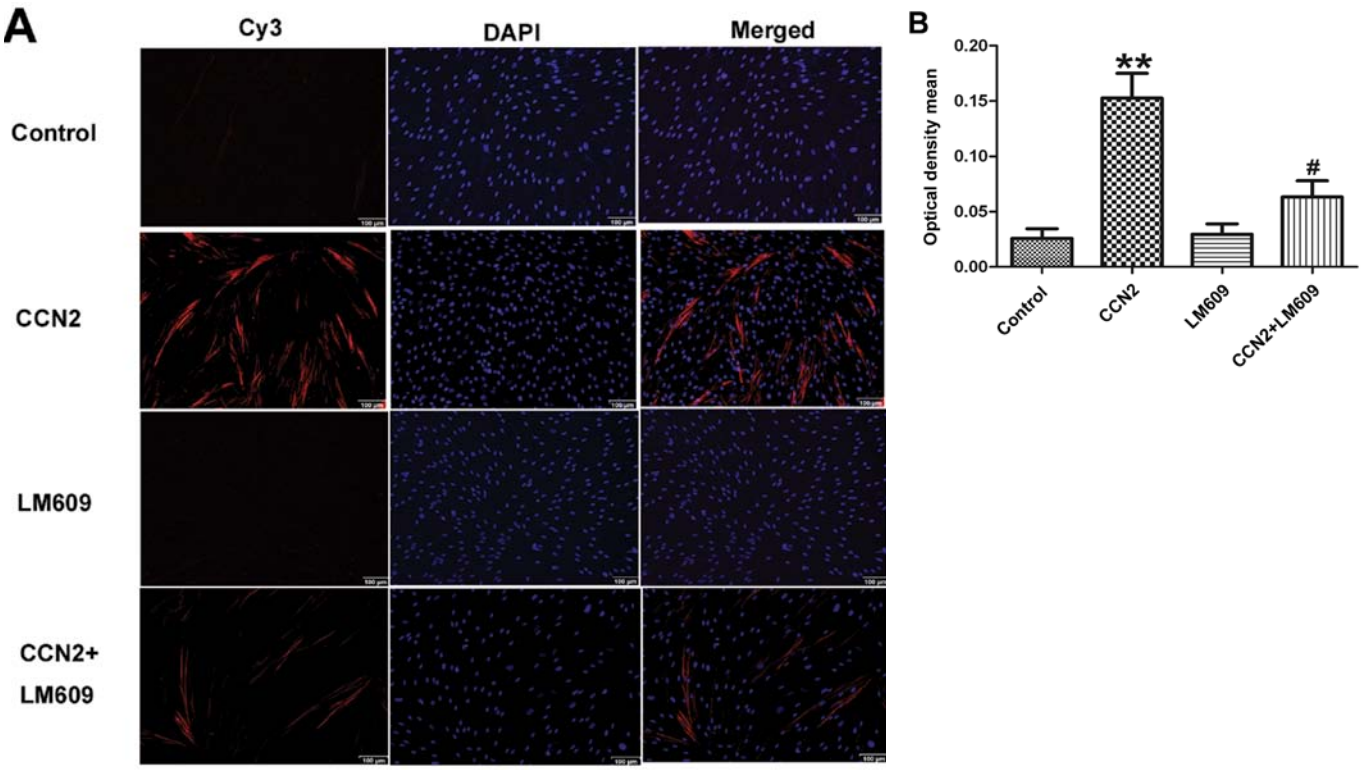

Figure 10. Effect of LM609 on the expression of α-smooth muscle actin (SMA) induced by CCN2 in hypertrophic scar fibroblasts (HTSF). HTSFs were pretreated with integrin $\alpha_v\beta_3$ antibody (LM609, 10 μg/ml) for 1 h. Subsequently, they were treated with CCN2 (40 ng/ml) for 48 h. Expression of α-SMA were determined by immunocytochemical analysis. (A) LM609 markedly suppressed CCN2-induced α-SMA expression by immunocytochemistry. (B) Quantification of the optical density of the immunocytochemical staining for α-SMA. Data are representative of three independent experiments. **P<0.01 vs. control; $^{\#}$p<0.05 vs. CCN2 group.

and COL III. Moreover, SB431542 significantly inhibited the expression of α-SMA COL I and COL III compared with LM609 (Figs. 11 and 12).

LM609-mediated blockade of CCN2 inhibited the contractility of HTSF. To determine whether the CCN2-induced changes in α-SMA protein and their inhibition by LM609 had functional consequences, the fibroblast-populated COL lattices (FPCLs) contraction assay was performed. As a model of a three-dimensional wound environment, HTSFs were embedded in COL matrices attached to the culture plate to generate FPCL in the presence of CCN2. HTSFs in mechanically stretched microenvironments have their cytoskeletons remodeled and exhibit a contractive phenotype (20). In our study model, CCN2 treatment (40 ng/ml) induced a significant (p<0.05) increase in contraction compared to the control

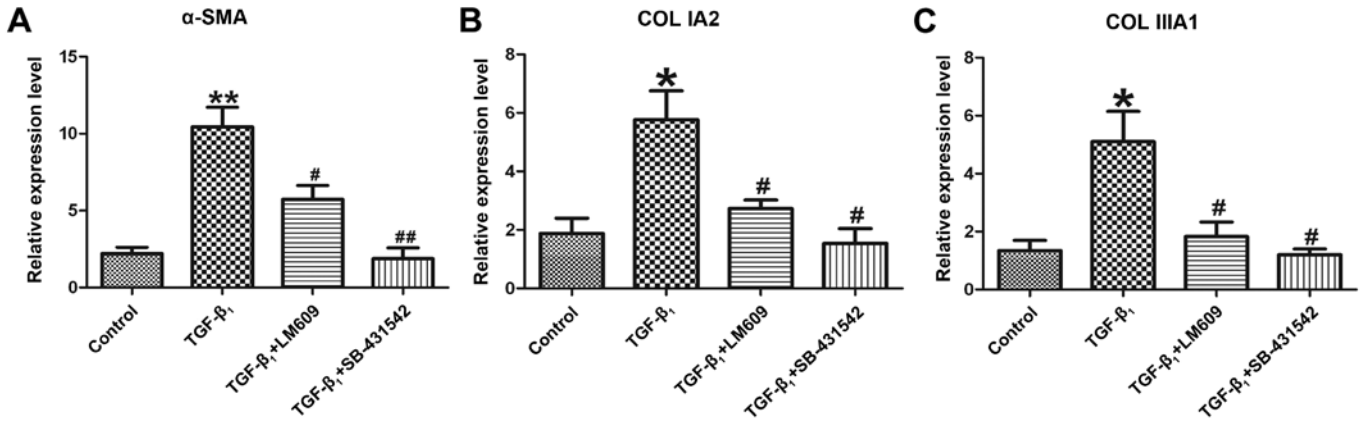

Figure 11. Hypertrophic scar fibroblasts (HTSFs) are controlled by blockage of the integrin receptor after TGF-β_1 stimulation. HTSFs were pretreated with integrin $\alpha_v\beta_3$ antibody (LM609, 10 μg/ml) or activin receptor-like kinase (ALK)5 inhibitor (SB431542, 10 μM) for 1 h. Subsequently, they were treated with TGF-β_1 (10 ng/ml) for 24 h. Expression of α-smooth muscle actin (SMA), collagen (COL) IA2 and COL IIIA1 was determined by qPCR. (A) α-SMA, (B) COL IA2 and (C) COL IIIA1. Data are representative of three independent experiments. *P<0.05 vs. control, **p<0.01 vs. control; $^{\#}$p<0.05 vs. TGF-β_1 group, $^{\#\#}$p<0.01 vs. TGF-β_1 group.

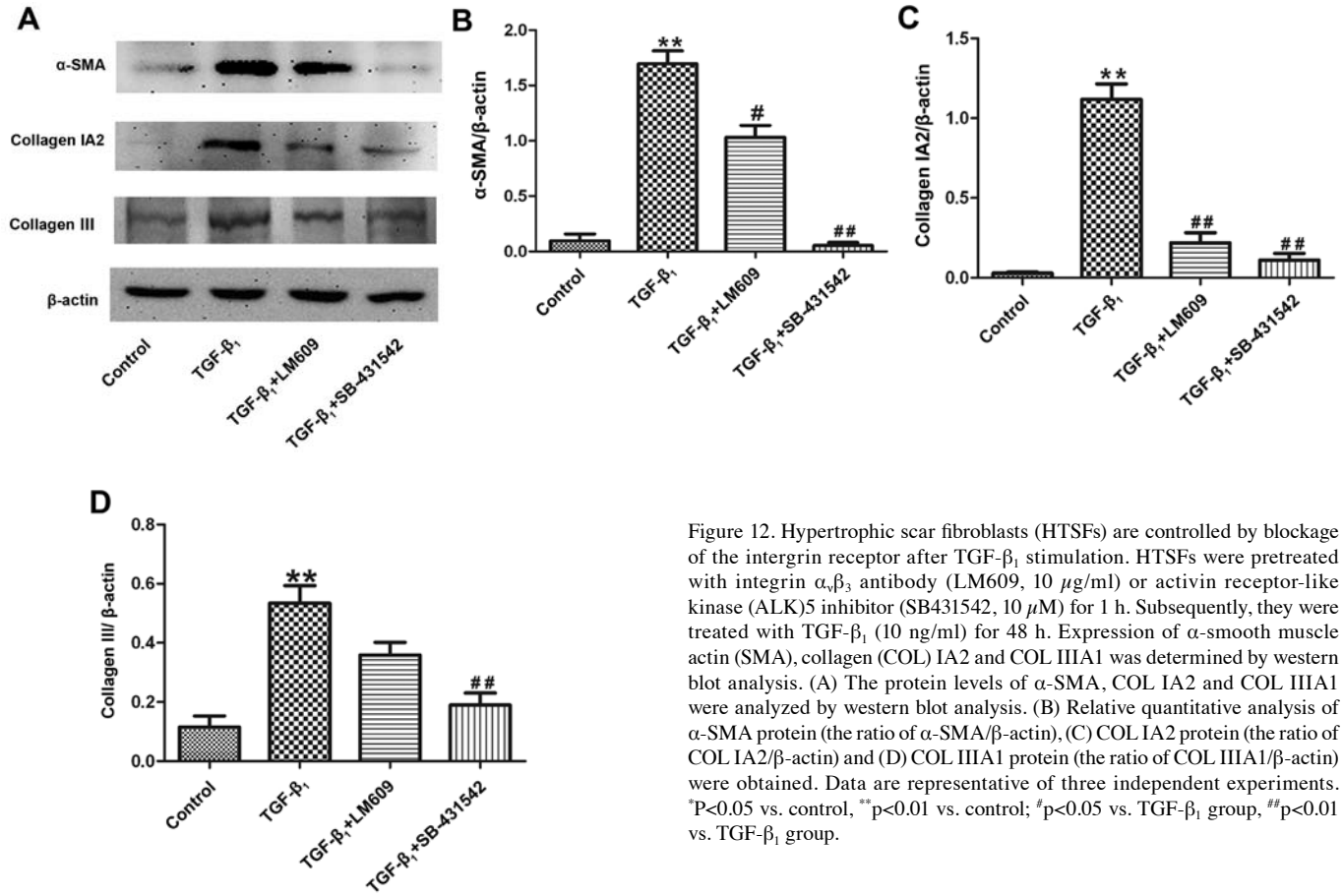

Figure 12. Hypertrophic scar fibroblasts (HTSFs) are controlled by blockage of the intergrin receptor after TGF-β_1 stimulation. HTSFs were pretreated with integrin $\alpha_v\beta_3$ antibody (LM609, 10 μg/ml) or activin receptor-like kinase (ALK)5 inhibitor (SB431542, 10 μM) for 1 h. Subsequently, they were treated with TGF-β_1 (10 ng/ml) for 48 h. Expression of α-smooth muscle actin (SMA), collagen (COL) IA2 and COL IIIA1 was determined by western blot analysis. (A) The protein levels of α-SMA, COL IA2 and COL IIIA1 were analyzed by western blot analysis. (B) Relative quantitative analysis of α-SMA protein (the ratio of α-SMA/β-actin), (C) COL IA2 protein (the ratio of COL IA2/β-actin) and (D) COL IIIA1 protein (the ratio of COL IIIA1/β-actin) were obtained. Data are representative of three independent experiments. *P<0.05 vs. control, **p<0.01 vs. control; $^{\#}$p<0.05 vs. TGF-β_1 group, $^{\#\#}$p<0.01 vs. TGF-β_1 group.

untreated cells after 48 h. When LM609 was added to the gels at the same time as CCN2, CCN2-induced gel contraction was blocked (Fig. 13). To evaluate the whether the change of the contractility was associated with α-SMA expression, the total RNA of the HTSF in the COL lattices was extracted and qPCR was conducted. Similar to the results above, the fibroblasts cultured in the three-dimensional environment showed an increased expression of α-SMA mRNA after CCN2 stimulation, which was inhibited by LM609 (Fig. 13C). Additionally, H&E staining results showed the architecture of FPCL. Of note, in the CCN2 + LM609 treatment groups, the architecture of FPCL was significantly improved compared with the CCN2 activation group (Fig. 14).

Effects of CCN2 and $\alpha_v\beta_3$ integrin-specific inhibitor on HTS in the rabbit ear scar model. On day 56 post-wounding,

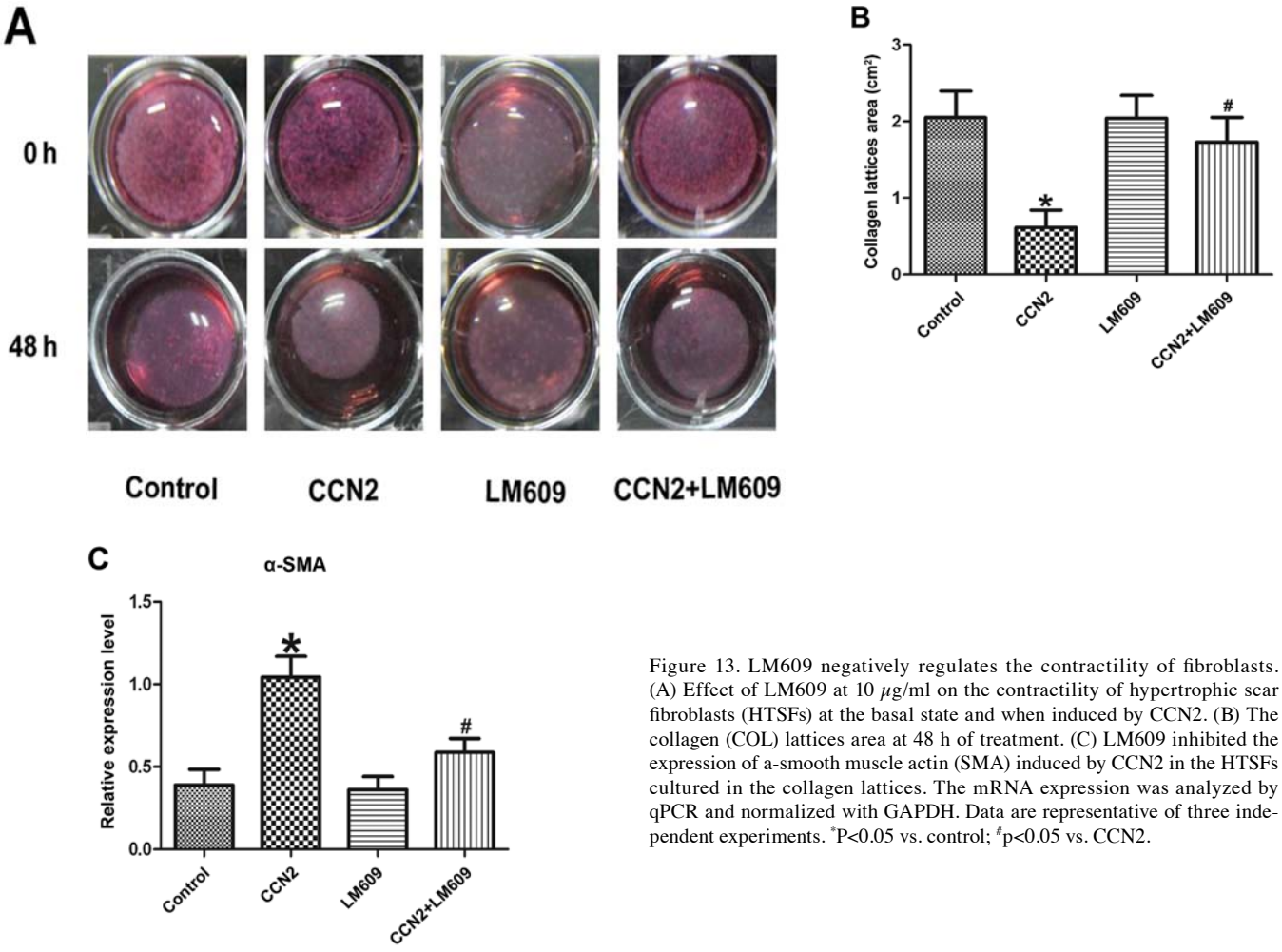

Figure 13. LM609 negatively regulates the contractility of fibroblasts. (A) Effect of LM609 at 10 μg/ml on the contractility of hypertrophic scar fibroblasts (HTSFs) at the basal state and when induced by CCN2. (B) The collagen (COL) lattices area at 48 h of treatment. (C) LM609 inhibited the expression of a-smooth muscle actin (SMA) induced by CCN2 in the HTSFs cultured in the collagen lattices. The mRNA expression was analyzed by qPCR and normalized with GAPDH. Data are representative of three independent experiments. *P<0.05 vs. control; $^{\#}$p<0.05 vs. CCN2.

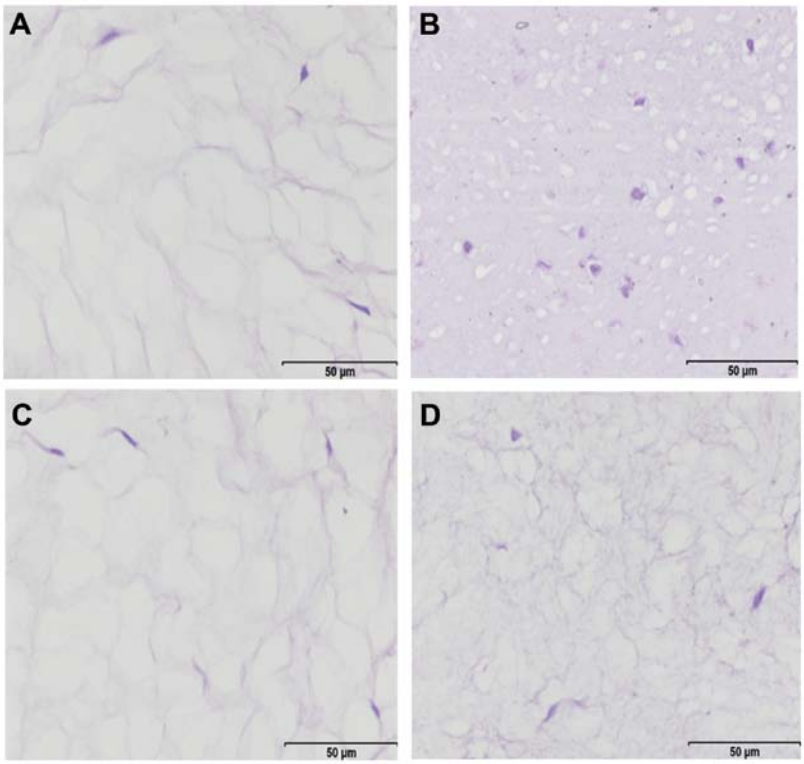

Figure 14. LM609 improves the architecture of FPCL. Following detachment from the surface of the well at 48 h, the gels were fixed and stained by hematoxylin and eosin (H&E) staining method. Scar bars 50 μm. (A) Non-treated control group, (B) CCN2 (40 ng/ml)-treated group, (C) LM609 (10 μg/ml)-stimulated group and (D) CCN2 (40 ng/ml) + LM609 (10 μg/ml)-treated group.

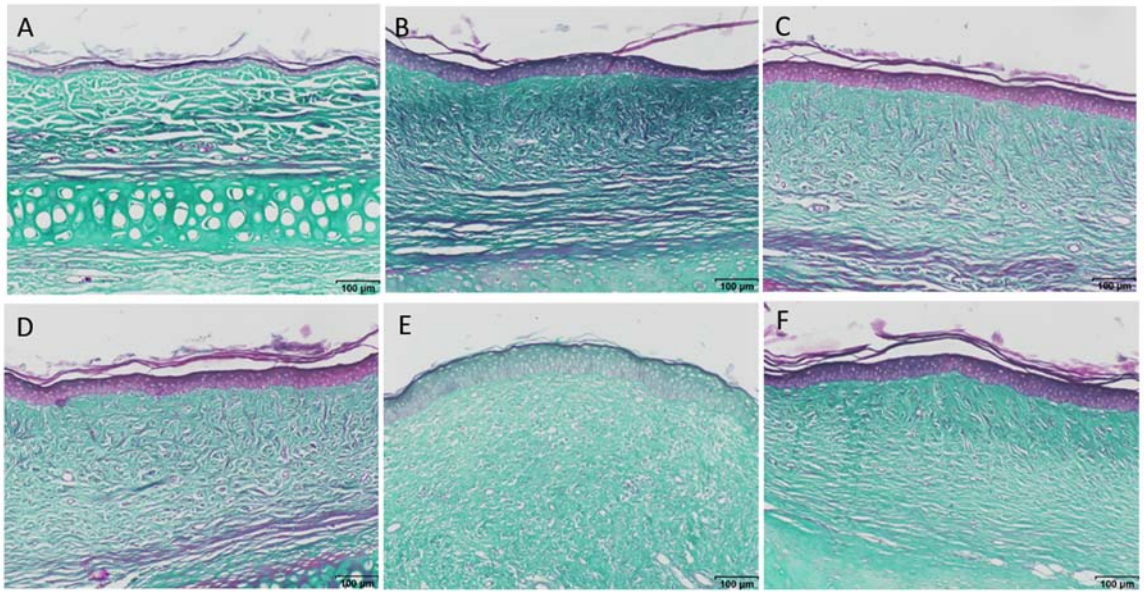

Figure 15. Masson's trichrome staining findings for collagen (COL). (A) Unwounded (normal) skin with regularly arranged, small COL fibers. (B-D) In the control, PBS and CCN2 groups, the amount of COL fibers is far more than that in the normal group, and collagen fibers are thicker, denser and disorganized. (E-F) After treatment with (E) CCN2 + LM609 and (F) LM609 for 28 days, the COL fibers were arranged more regularly and sparsely than those in the control, PBS and CCN2 groups (n=18 scars per group). Bars 100 μm.

significant hypertrophic scarring was evident in the control, PBS and CCN2 groups. Overproduction of COL is a major characteristic of HTSs. Thus, Masson's trichrome staining of scar tissue was performed on day 56 post-wounding. Light microscopy revealed more features typical of COL fibers in scar tissue (Fig. 15B-D) in the control group compared with unwounded dermal tissue (Fig. 15A). The COL bundles were more abundant, denser, thicker and disorganized. By contrast, the COL fibers in the groups treated with CCN2 + LM609 and LM609 were fewer, thinner and more regularly arranged (Fig. 15E and F).

Discussion

Hypertrophic scarring is a common complication of wound healing. It is associated with an abnormal proliferation of fibroblasts and an overproduction of COL and other ECM elements. Fibroblast proliferation and matrix synthesis induced by growth factors have been considered to be involved in initiating and maintaining fibrosis (24). Although the underlying mechanisms involved are complex, different effects of CCN2 mediate many harmful aspects of hypertrophic scarring.

CCN2 has been involved in many fibrotic disorders of the lung, liver, kidney and pancreas. Treatment with antisense oligonucleotides or antibodies to CCN2 in cell culture or animal models decreased ECM synthesis and reduced scarring (13,25-27). Moreover, CCN2 mediates the fibroproliferative effects of TGF-β_1. Levels of CCN2 are correlated with an increased expression of ECM, such as COL I, integrins and fibronectin. Therefore, it is important to define the signaling pathway through CCN2 (28). Constitutive CCN2 expression is a hallmark of fibrosis (29). In adults, CCN2 is induced during tissue repair (30). Simultaneous co-injection of CCN2 and TGF-β causes sustained fibrotic responses *in vivo*, in contrast to the application of TGF-β alone, which causes only a transient fibrotic response that depends on the constant injection of ligand (31). In general, the biological effect of cytokines is mainly determined by the occurrence of cytokine-receptor interaction, which is modulated by the concentration and activity of cytokines and/or their receptors. For example, in scleroderma fibroblasts, the upregulated expression of TGF-β receptors contributes to the increased biological effect of autocrine TGF-β, resulting in excessive ECM deposition (32). Integrin $\alpha_v\beta_3$ plays an important role in a variety of physiological and patho-physiological processes, including tumor angiogenesis, rheumatoid arthritis and a number of inflammatory and repair processes (33). Integrin $\alpha_v\beta_3$ has been shown to bind CCN2 proteins. Previously, it was shown that integrin $\alpha_v\beta_3$ function as co-receptors with heparan sulfate proteoglycans (HSPGs) for CCN2-mediated hepatic stellate cell adhesion (34).

In the present study, we found that the mRNA levels of integrin α_v and β_3 increased in HTS. In HTSF, the expression of integrin α_v and β_3 mRNA was also significantly increased (Fig. 3). CCN2 stimulation of HTSF resulted in upregulation of the cell expression of α-SMA, COL IA2, and COL IIIA1, which are important components of the ECM in skin tissue (Figs. 5 and 6). In addition, we detected increased expression levels of integrin α_v and β_3 subunits during the transition (Fig. 7).

Integrin α_v is involved in differentiation in a variety of cell types, including osteoclasts, oligodendrocytes, keratinocytes and myoblasts (35-38). In scleroderma fibroblasts, integrin $\alpha_v\beta_5$ is upregulated and was shown to be capable of interacting with TGF-β receptors. Furthermore, the blockade of integrin $\alpha_v\beta_5$ reversed the myofibroblastic phenotype in scleroderma fibroblasts (39). In our experiments, treatment of HTSF cells with the $\alpha_v\beta_3$ integrin-specific inhibitor (LM609) significantly reduced

the cell expression of α-SMA and COL IA2, while immunocytochemistry demonstrated that LM609 led to suppression of the CCN2-induced expression of α-SMA (Figs. 8-10).

HTSF can be controlled by blockage of the integrin receptor following TGF-β_1 stimulation because it has been demonstrated that an increased TGF-β_1 occurs in HTS *in vitro* and *in vivo*. To confirm this, we detected the expression level of α-SMA COL I and COL III in HTS fibroblasts treated with different receptor inhibitors following TGF-β_1 stimulation. The data showed that compared with the control, TGF-β_1 markedly stimulated α-SMA COL I and COL III expression, while the treatment with ALK5 inhibitor (SB431542) and $\alpha_v\beta_3$ integrin-specific inhibitor (LM609) suppressed the TGF-β_1-induced expression of α-SMA, COL I and COL III. Moreover, SB431542 significantly inhibited the expression of α-SMA COL I and COL III compared with LM609 (Figs. 11 and 12).

To validate our hypothesis, fibroblast-populated COL lattices contraction assays and a rabbit ear HTS model was established, and the role of integrin $\alpha_v\beta_3$ was investigated. In the FPCLs model, the integrin $\alpha_v\beta_3$-specific inhibitor (LM609) blocked the CCN2-induced increase in contractility of the HTSFs, suggesting that LM609 may negatively regulate the contractility of HTSFs. Furthermore, the fibroblasts cultured in the three-dimensional environment showed an increased expression of α-SMA mRNA after CCN2 stimulation, which was inhibited by LM609. Additionally, the H&E staining results showed that the architecture of FPCL in the CCN2 + LM609 treatment groups was significantly improved compared with that of the CCN2 activation group (Figs. 13 and 14). In a rabbit ear HTS model, Masson staining revealed that the COL bundles were more abundant, denser, thicker, and disorganized in the control group. By contrast, there were fewer, thinner, and more organized COL fibers in the groups treated with CCN2 + LM609 and LM609 (Fig. 15). The results of this study suggest that $\alpha_v\beta_3$ integrin inhibition was able to significantly inhibit post-injury scarring of the model rabbit ears. These findings suggest that integrin $\alpha_v\beta_3$ is a key receptor for modulating the signals by which CCN2 promotes α-SMA and collagen expression in HTSF.

In summary, we have demonstrated that the upregulated expression of integrin α_v and β_3 induce myofibroblastic differentiation of HTSF. This finding may provide insights into the regulatory mechanisms of fibrotic disorders, such as HTS.

Acknowledgements

This study was supported by the Grant-in-Aid for scientific research from the Xijing hospital assist (XJZT13M16), and the National Natural Science Foundation of China (grant no. 81171811).

References

1. Gauglitz GG, Korting HC, Pavicic T, Ruzicka T and Jeschke MG: Hypertrophic scarring and keloids: pathomechanisms and current and emerging treatment strategies. Mol Med 17: 113-125, 2011.
2. Jun JI and Lau LF: Taking aim at the extracellular matrix: CCN proteins as emerging therapeutic targets. Nat Rev Drug Discov 10: 945-963, 2011.
3. Shi-Wen X, Leask A and Abraham D: Regulation and function of connective tissue growth factor/CCN2 in tissue repair, scarring and fibrosis. Cytokine Growth Factor Rev 19: 133-144, 2008.
4. de Winter P, Leoni P and Abraham D: Connective tissue growth factor: structure-function relationships of a mosaic, multifunctional protein. Growth Factors 26: 80-91, 2008.
5. Chen CC and Lau LF: Functions and mechanisms of action of CCN matricellular proteins. Int J Biochem Cell Biol 41: 771-783, 2009.
6. Phanish MK, Winn SK and Dockrell ME: Connective tissue growth factor-(CTGF, CCN2) - a marker, mediator and therapeutic target for renal fibrosis. Nephron Exp Nephrol 114: e83-e92, 2010.
7. Hu X, Wang H, Liu J, Fang X, Tao K, Wang Y, Li N, Shi J, Wang Y, Ji P, Cai W, Bai X, Zhu X, Han J and Hu D: The role of ERK and JNK signaling in connective tissue growth factor induced extracellular matrix protein production and scar formation. Arch Dermatol Res 305: 433-445, 2013.
8. Shi-wen X, Stanton LA, Kennedy L, Pala D, Chen Y, Howat SL, Renzoni EA, Carter DE, Bou-Gharios G, Stratton RJ, Pearson JD, Beier F, Lyons KM, Black CM, Abraham DJ and Leask A: CCN2 is necessary for adhesive responses to transforming growth factor-beta1 in embryonic fibroblasts. J Biol Chem 281: 10715-10726, 2006.
9. Colwell AS, Phan TT, Kong W, Longaker MT and Lorenz PH: Hypertrophic scar fibroblasts have increased connective tissue growth factor expression after transforming growth factor-beta stimulation. Plast Reconstr Surg 116: 1387-1390, 2005.
10. van der Veer WM, Bloemen MC, Ulrich MM, Molema G, van Zuijlen PP, Middelkoop E and Niessen FB: Potential cellular and molecular causes of hypertrophic scar formation. Burns 35: 15-29, 2009.
11. Wang J, Dodd C, Shankowsky HA, Scott PG and Tredget EE; Wound healing research group: Deep dermal fibroblasts contribute to hypertrophic scarring. Lab Invest 88: 1278-1290, 2008.
12. Nakerakanti SS, Bujor AM and Trojanowska M: CCN2 is required for the TGF-β induced activation of Smad1-Erk1/2 signaling network. PLoS One 6: e21911, 2011.
13. Sisco M, Kryger ZB, O'Shaughnessy KD, Kim PS, Schultz GS, Ding XZ, Roy NK, Dean NM and Mustoe TA: Antisense inhibition of connective tissue growth factor (CCN2/CCN2) mRNA limits hypertrophic scarring without affecting wound healing in vivo. Wound Repair Regen 16: 661-673, 2008.
14. Scaffidi AK, Petrovic N, Moodley YP, Fogel-Petrovic M, Kroeger KM, Seeber RM, Eidne KA, Thompson PJ and Knight DA: alpha(v)beta(3) integrin interacts with the transforming growth factor beta (TGFbeta) type II receptor to potentiate the proliferative effects of TGFbeta1 in living human lung fibroblasts. J Biol Chem 279: 37726-37733, 2004.
15. Asano Y, Ihn H, Yamane K, Jinnin M, Mimura Y and Tamaki K: Increased expression of integrin alpha(v)beta3 contributes to the establishment of autocrine TGF-beta signaling in scleroderma fibroblasts. J Immunol 175: 7708-7718, 2005.
16. Cruet-Hennequart S, Maubant S, Luis J, Gauduchon P, Staedel C and Dedhar S: Alpha(v) integrins regulate cell proliferation through integrin-linked kinase (ILK) in ovarian cancer cells. Oncogene 22: 1688-1702, 2003.
17. Levinson H, Hopper JE and Ehrlich HP: Overexpression of integrin alphav promotes human osteosarcoma cell populated collagen lattice contraction and cell migration. J Cell Physiol 193: 219-224, 2002.
18. Meerovitch K, Bergeron F, Leblond L, Grouix B, Poirier C, Bubenik M, Chan L, Gourdeau H, Bowlin T and Attardo G: A novel RGD antagonist that targets both alphavbeta3 and alpha5beta1 induces apoptosis of angiogenic endothelial cells on type I collagen. Vascul Pharmacol 40: 77-89, 2003.
19. Trusolino L, Serini G, Cecchini G, Besati C, Ambesi-Impiombato FS, Marchisio PC and De Filippi R: Growth factor-dependent activation of alphavbeta3 integrin in normal epithelial cells: implications for tumor invasion. J Cell Biol 142: 1145-1156, 1998.
20. Liu J, Wang Y, Pan Q, Su Y, Zhang Z, Han J, Zhu X, Tang C and Hu D: Wnt/β-catenin pathway forms a negative feedback loop during TGF-β1 induced human normal skin fibroblast-to-myofibroblast transition. J Dermatol Sci 65: 38-49, 2012.
21. Shi JH, Guan H, Shi S, Cai WX, Bai XZ, Hu XL, Fang XB, Liu JQ, Tao K, Zhu XX, Tang CW and Hu DH: Protection against TGF-β1-induced fibrosis effects of IL-10 on dermal fibroblasts and its potential therapeutics for the reduction of skin scarring. Arch Dermatol Res 305: 341-52, 2013.
22. Bell E, Ivarsson B and Merrill C: Production of a tissue-like structure by contraction of collagen lattices by human fibroblasts of different proliferative potential in vitro. Proc Natl Acad Sci USA 76: 1274-1278, 1979.

23. Sarrazy V, Billet F, Micallef L, Coulomb B and Desmoulière A: Mechanisms of pathological scarring: role of myofibroblasts and current developments. Wound Repair Regen 19 (Suppl 1): s10-s15, 2011.
24. Gurtner GC, Werner S, Barrandon Y and Longaker MT: Wound repair and regeneration. Nature 453: 314-21 2008.
25. Leask A and Abraham DJ: All in the CCN family: essential matricellular signaling modulators emerge from the bunker. J Cell Sci 119: 4803-4810, 2006.
26. Luft FC: CCN2, the connective tissue growth factor. J Mol Med (Berl) 86: 1-3, 2008.
27. Wang Q, Usinger W, Nichols B, Gray J, Xu L, Seeley TW, Brenner M, Guo G, Zhang W, Oliver N, Lin A and Yeowell D: Cooperative interaction of CCN2 and TGF-β in animal models of fibrotic disease. Fibrogenesis Tissue Repair 4: 4, 2011.
28. Leask A and Abraham DJ: The role of connective tissue growth factor, a multifunctional matricellular protein, in fibroblast biology. Biochem Cell Biol 81: 355-63, 2003.
29. Blom IE, Goldschmeding R and Leask A: Gene regulation of connective tissue growth factor: new targets for antifibrotic therapy? Matrix Biol 21: 473-482, 2002.
30. Igarashi A, Okochi H, Bradham DM and Grotendorst GR: Regulation of connective tissue growth factor gene expression in human skin fibroblasts and during wound repair. Mol Biol Cell 4: 637-645, 1993.
31. Mori T, Kawara S, Shinozaki M, Hayashi N, Kakinuma T, Igarashi A, Takigawa M, Nakanishi T and Takehara K: Role and interaction of connective tissue growth factor with transforming growth factor-beta in persistent fibrosis: a mouse fibrosis model. J Cell Physiol 181: 153-159, 1999.
32. Ihn H, Yamane K, Kubo M and Tamaki K: Blockade of endogenous transforming growth factor beta signaling prevents up-regulated collagen synthesis in scleroderma fibroblasts: association with increased expression of transforming growth factor beta receptors. Arthritis Rheum 44: 474-480, 2001.
33. Miller WH, Keenan RM, Willette RN and Lark MW: Identification and in vivo efficacy of small-molecule antagonists of integrin alphavbeta3 (the vitronectin receptor). Drug Discov Today 5: 397-408, 2000.
34. Gao R and Brigstock DR: Connective tissue growth factor (CCN2) induces adhesion of rat activated hepatic stellate cells by binding of its C-terminal domain to integrin alpha(v)beta(3) and heparan sulfate proteoglycan. J Biol Chem 279: 8848-8855, 2004.
35. Blaschuk KL, Guérin C and Holland PC: Myoblast alphav beta3 integrin levels are controlled by transcriptional regulation of expression of the beta3 subunit and down-regulation of beta3 subunit expression is required for skeletal muscle cell differentiation. Dev Biol 184: 266-277, 1997.
36. Milner R, Huang X, Wu J, Nishimura S, Pytela R, Sheppard D and ffrench-Constant C: Distinct roles for astrocyte alphavbeta5 and alphavbeta8 integrins in adhesion and migration. J Cell Sci 112: 4271-4279, 1999.
37. Rodan SB and Rodan GA: Integrin function in osteoclasts. J Endocrinol 154: S47-S56, 1997.
38. Thomas GJ, Lewis MP, Hart IR, Marshall JF and Speight PM: AlphaVbeta6 integrin promotes invasion of squamous carcinoma cells through up-regulation of matrix metalloproteinase-9. Int J Cancer 92: 641-650, 2001.
39. Asano Y, Ihn H, Yamane K, Jinnin M and Tamaki K: Increased expression of integrin alphavbeta5 induces the myofibroblastic differentiation of dermal fibroblasts. Am J Pathol 168: 499-510, 2006.